

# Effects of charge distribution on water filling process in carbon nanotube

MENG LingYi<sup>1</sup>, LI QiKai<sup>1†</sup> & SHUAI ZhiGang<sup>1,2†</sup><sup>1</sup> Beijing National Laboratory for Molecular Sciences and Key Laboratory of Organic Solids, Institute of Chemistry, Chinese Academy of Sciences, Beijing 100190, China;<sup>2</sup> Department of Chemistry, Tsinghua University, Beijing 100084, China

**Using umbrella sampling technique with molecular dynamics simulation, we investigated the nanofluidic transport of water in carbon nanotube (CNT). The simulations showed that a positive charge modification to the carbon nanotube can slow down the water column growth process, while the negative charge modification to the carbon nanotube will, on the other hand, quicken the water column growth process. The free energy curves were obtained through the statistical process of water column growth under different charge distributions, and the results indicated that these free energy curves can be employed to explain the dynamical process of water column growth in the nanosized channels.**

nanotube, micro/nanofluidic, molecular dynamics

## 1 Introduction

Owing to the many unique properties, carbon nanotubes (CNTs) have been extensively investigated as artificial nanopores and ion channels mimicking the vital membrane structure in cells<sup>[1,2]</sup> or providing a prototype for designing of desalination devices<sup>[3]</sup>. In biological system, the nanosized pores for transporting water are essential for living organisms ranging from bacteria to animals and plants<sup>[4]</sup>. However, the biological water channels are much more complex than CNTs, for example, with irregular surfaces and highly inhomogeneous charge distributions. Even with the above shortcomings, the CNTs can still be protonated<sup>[5]</sup>, and some may have charged atomic sites<sup>[6]</sup> to closely mimic the real structures. Reports of rapid water conduction through the narrow (6, 6) carbon nanotubes, however, are particularly intriguing as these may be promising for forming semipermeable membranes that filter salt from water<sup>[2]</sup>. Further studies showed that when the CNT was modified through charged atoms, new distribution or structure patterns and controllable transport of water can be realized<sup>[1,7,8]</sup>.

Recent theoretical studies<sup>[9]</sup> and computer simulations<sup>[10–12]</sup> have demonstrated that the confined water is thermodynamically different from the bulk water, and the structure and dynamics of the nanoconfined water in particular have received considerable attention<sup>[13–18]</sup>. Computational studies have been conducted for structural properties of water molecules inside and near the CNTs, finding that water tends to form very ordered structures inside and at the mouth of pores<sup>[2, 14, 19–21]</sup>. As described above, there have been some studies aiming at determining the conductance of water through CNTs<sup>[1,2]</sup>. The structure of water droplets<sup>[22]</sup> or clusters<sup>[23]</sup> confined at the nanometer scale and the capillary effects<sup>[24]</sup> have also been explored. The investigation of these size-constraint systems not only can help us understand the structural and dynamic properties of those media

Received October 6, 2008; accepted November 18, 2008

doi: 10.1007/s11426-009-0016-0

†Corresponding author (email: qkli@iccas.ac.cn, zgshuai@iccas.ac.cn)

Supported by the National Natural Science Foundation of China (Grant Nos. 10425420 and 20773145), the Ministry of Science and Technology of China (Grant Nos. 2006CB806200 and 2006CB932100), and the Chinese Academy of Sciences including its CNIC Supercomputer Center.

confined on the nanometer scale, but also can reveal some special characters of the nanosized materials, the hydrophobic/hydrophilic behavior in particular<sup>[25–28]</sup>. Hydrophilic/hydrophobic effects at the nanometer scale play a key role in many important physical or chemical phenomena, such as self-assembly and controllable growth of nanosized materials, stabilization of protein structure and function in solvent.

To understand the underlying structure and dynamic features at the nanometer scale, we resort to the potential of mean force (PMF) analysis. However, the standard simulation methods do not adequately sample the region to which the system reaches with low probability. For example, in our previous work<sup>[19]</sup>, we calculated a series of PMF curves used to provide an estimation over the relative energy barriers for the water molecules entering into the channels and gain some insight into the structural information of water clusters in the stable stage for CNTs with different sizes. The study of the water filling process in carbon nanotubes can enhance our understanding on the formation of the quite surprising structures like the so-called quasi-one-dimensional liquid water in the case of the narrow (6, 6) CNT<sup>[13]</sup>. This can be related with the fact that the forces acting on the water molecules destined to enter the narrow tubes are greater than those of the wider tubes. However, obtaining the dynamical properties of the water filling process is not feasible by those calculations as the low probability events can not be effectively sampled. To avoid the sampling problem, various methods have been proposed for calculating the PMF, for instance, the umbrella sampling and the steered dynamics<sup>[29]</sup>. If applicable, umbrella sampling combined with the weighted histogram analysis method (WHAM) is perhaps the best choice for calculating the PMF<sup>[30]</sup>. Umbrella sampling is a technique frequently employed in computational physics and chemistry, and is used to improve sampling of a system (or different systems) where ergodicity is hindered by the system's energy landscape. It was first suggested by Torrie and Valleau<sup>[31]</sup> in 1977, and the umbrella sampling method can be very efficient in sampling low probability events.

In this paper, the water column growth inside the CNTs with various charge placements and indenting depths, and their variations with the evolution time are studied. The free energy curves in the process of water column growth are obtained by using the umbrella sam-

pling coupled with WHAM, and analyses are made in the dynamical process of water column growth in the nanosized channel by employing these free energy curves. Rather than by taking advantage of the deformation of CNT as a control mechanism as proposed by Wan et al.<sup>[32]</sup>, in this paper we hope to constitute an effective method to control the water filling process in CNT and gain some insight into the CNT-based nanoscale devices.

## 2 Simulation model and computational details

Our simulations were performed by using the GROMACS molecular dynamics package<sup>[33,34]</sup>. The water is described by the flexible SPC/E model featuring harmonic stretch and bend terms between the oxygen and hydrogen atoms at which the partial charges are located, and the electrostatic interactions are evaluated by the particle mesh Ewald (PME) method<sup>[35,36]</sup>. The force fields and parameters utilized in the simulation are the same as those described in ref. [19]. The single-walled carbon nanotube (SWNT)-water system is modeled using the canonical (NVT) ensemble, and the periodic boundary conditions are applied in all the three spatial directions. However, enough space (around 3.8 nm) is left between the top of SWNT and the bottom-clamped water layer along  $z$  direction to avoid unreasonable interaction. The temperature is maintained at 300 K using the Berendsen method. A time step of 1.0 fs is used. The cutoff distances for Coulomb potential and Lennard-Jones potential are 0.9 nm and 1.0 nm respectively.

The simulations were carried out as follows: an uncapped (6, 6) single-walled nanotube (SWNT) of about 4 nm in length and with various charge distributions is dipped into water surface as a function of cosine-type (stage 1), then the system holds and relaxes at the maximal dipping position (stage 2). To realize this process, we first froze a layer of water molecules at the bottom of the bath (about 1 nm in thickness) and the top part of the SWNT (about 1 nm in length) as shown in Figure 1. It takes about 100 ps for the SWNT to be fully immersed into its maximal depth under water surface, and the maximal depths are around 2.0 nm and 3.0 nm. The coordinates and other information were recorded every 0.2 ps. The water box with 12258 molecules is prepared separately, and the system is equilibrated to

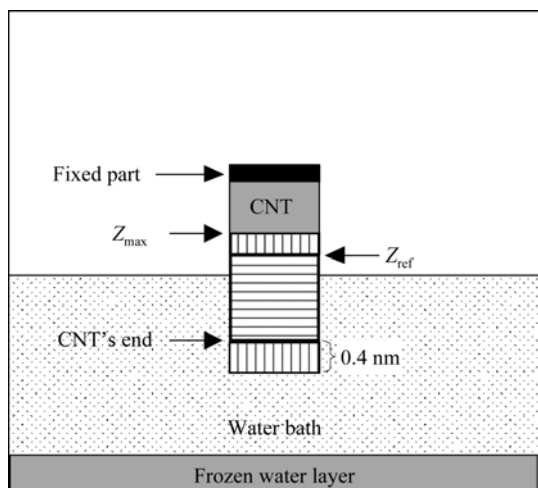


**Figure 1** A schematic of the MD simulation system and the regions for applying the umbrella potential calculations. The vertical hatched areas correspond to possible operation zones for the umbrella potential calculations.

obtain the desired temperature ( $T$ ) of 300 K. The dimension of the water box is approximately  $8 \text{ nm} \times 8 \text{ nm} \times 6 \text{ nm}$ . To investigate the charge effects, we further decorated the SWNTs by placing equal partial charges on the terminated carbon atoms at the lower end of SWNTs. The magnitude of the average partial charge (when water is included in the tube) on terminated carbon atom of the (6, 6) SWNT is calculated by using the Gaussian03<sup>[37]</sup> program package at the B3LYP/6-31G\*\* level and this quantum value is about  $0.08 e$ <sup>[38]</sup>, which was set as  $0.1 e$  in this simulation. For comparison, another charge value  $0.3 e$  corresponding to the (10, 0) CNT with similar diameter to that of the (6, 6) CNT<sup>[38]</sup> is also used to decorate the SWNTs in this paper. As a result, there are four types of charged SWNTs in this simulation, and the partial charges placed on the terminated carbon atoms at the lower end of SWNTs are respectively  $+0.3 e$ ,  $+0.1 e$ ,  $-0.1 e$  and  $-0.3 e$ . It should be noticed that the polarization effect is neglected by using the fixed charges of moving atoms during MD simulation, and this will lead to the insufficiency in sampling the phase space when calculating the changes in free energy. To neutralize the net charges for the overall system, dummy particles with opposite partial charges are fixed at the location far away from the interesting regions.

During the process of umbrella sampling, the water column length inside the SWNT is chosen as the order

parameter and the range of its values ( $0-4 \text{ nm}$ ) is divided into  $N_w$  sampling windows centered around the conveniently chosen values  $Z_{ref, i}$ ,  $i = 1, \dots, N_w$ . There are a total of eleven sampling windows ( $N_w=11$ ) in the simulations, and the window size is chosen to be  $0.4 \text{ nm}$  (slightly larger than the dimension of one water molecule). The umbrella potential assumes a quadratic form:

$$V_{umb} = \frac{1}{2} k_z (Z_{max} - Z_{ref})^2, \quad (1)$$

where  $k_z = 25.0 \text{ kJ} \cdot \text{mol}^{-1} \cdot \text{nm}^{-2}$ . The total excess force from umbrella potential is divided by the number of water molecules in the operational zone and then uniformly distributed over these water molecules. If the water column height  $Z_{max}$  is larger than the reference value of umbrella sampling  $Z_{ref}$ , all water molecules inside SWNT with  $Z > Z_{ref}$  are in the operational zone. However, if the water column height  $Z_{max}$  is lower than  $Z_{ref}$ , then the operational region is the vestibule extending from the SWNT's lower end into the bulk water by around  $0.4 \text{ nm}$  as shown in Figure 1. Through distributing the umbrella force solely on molecules in both the top and bottom operational regions, the probability of breaking the hydrogen-bonding network formed by water molecules inside SWNTs is greatly reduced, and at the same time the composition of those divided forces from umbrella potential can maintain a harmonic function of the column length. It takes around 200 ps to stabilize the initial conformations near each target reference  $Z_{ref, i}$  for sequential umbrella sampling, and the production run lasts over 800 ps.

The standard method for efficiently stitching together the biased distribution function  $p_i(Z)$ 's in order to obtain the equilibrium distribution function of the order parameter  $p_0(Z)$  is used, and therefore the sought free energy curve is the WHAM, according to eqs. (2) and (3):

$$p_0(Z) = \frac{\sum_{i=1}^{N_w} N_i p_i(Z)}{\sum_{i=1}^{N_w} N_i e^{-V_i(Z)} / \langle e^{-V_i} \rangle}, \quad (2)$$

$$\langle e^{-V_i} \rangle = \int dZ p_0(Z) e^{-V_i(Z)}, \quad (3)$$

where  $N_i$  is the number of data points used to construct the  $p_i(Z)$  for the  $i$ th sampling window. The above nonlinear coupled WHAM equations need to be solved iteratively and thus minimize the errors in determining the  $p_0(Z)$ . The free energy is calculated as

$$G(Z) = -k_B T \ln[p_0(Z)]. \quad (4)$$

### 3 Results and discussion

In the post-growth stage (lasting for 10 ns after about 2 ns in our simulations) of the water filling process into the SWNT, it is common that the water column inside the SWNT would fluctuate around the saturation height. However, in the case of SWNT with  $-0.1 e$  charge distribution, the water column saturation height inside SWNT is lower than the heights of SWNTs with the other charge distributions, and it also features larger fluctuation in height as shown in Table 1. In addition, the formation of a one-dimensionally ordered chain of water molecules is also observed in SWNTs decorated with partial charges. When the partial charges are large enough, there exist some orientational hydrogen-bonding defects near the charged carbon atomic sites, as shown in Figure 2. For example, in the case of  $+0.3 e$  charge distribution, the dipole moment of water molecule near the charged carbon atomic sites is perpendicular to the CNT axis, and the attracted oxygen atom gets more close to the CNT wall, while the two hydrogen atoms connect with other neighboring water molecules to form the hydrogen bond. Similarly, in the case of  $-0.3 e$  charge distribution, the dipole moment of water molecule near the charged carbon atomic sites is also perpendicular to the CNT axis, however, on the contrary, it is the oxygen atom that connects with other neighboring water molecules to form the hydrogen bond, while the two attracted hydrogen atoms get more close to the CNT wall. These structural features will prove reasonable by further analyzing the electrostatic force imposed on the water molecule near the charged carbon atomic sites of SWNT's wall. For these two cases, the oxygen atoms of water molecules near the charged carbon atomic sites are pulled away from the CNT axle by about  $1.6 \text{ \AA}$ . However, formations of the orientational hydrogen-bonding defects are less obvious for water chain structures inside SWNTs decorated with relatively less partial charges (for example,  $\pm 0.1 e$  in this simulation). Thus, it seems that the electrical field intensity must be high enough in order to form these special hydrogen-bonding defects. All these water structures in cases involved in charge distribution are more stable than those formed inside the pristine SWNT, and no collective flip (the angle of water dipole moment with the  $z$  axle changes from angle  $< 90^\circ$  to angle  $> 90^\circ$  or vice versa) inside charged SWNTs is observed during the long evolution process.

**Table 1** The saturation heights and error estimations for water column inside the SWNTs with various charge distributions and indenting depths<sup>a)</sup>

Type	+0.3 e	+0.1 e	0.0 e	-0.1 e	-0.3 e	+0.3 e*
Height (nm)	3.750	3.667	3.677	3.354	3.853	3.715
Error (nm)	0.1900	0.1966	0.2668	0.5930	0.1171	0.1696

a) The value marked with \* is corresponding to depth of 3.0 nm.

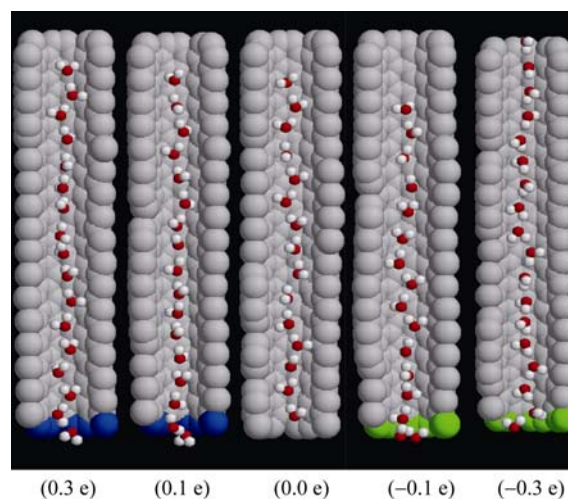


**Figure 2** The simulation snapshots of water molecules inside the SWNTs decorated with various charge distributions in the post-growth stage (after about 2 ns). The red balls represent oxygen atoms, the white balls the hydrogen atoms, the blue balls the positively charged carbon atoms and the green balls the negatively charged carbon atoms.

The effects of various charge distributions are systematically studied in the simulations. Figure 3 shows the average dipole moment angular distribution for water molecules near the vicinity to the lower end of SWNT along the  $z$  direction. The curve for the pristine SWNT was derived from the period in which the water molecules inside SWNT maintain the upward configuration. It is no doubt that in the case of  $-0.1 e$  charge distribution, the water molecules can easily enter into the mouth range of the SWNT, since the water molecules can smoothly adjust their dipole moment orientation near the mouth range of the SWNT to diffuse into the SWNT. On the other hand, in the case of charge distributions other than the  $-0.1 e$  distribution, more drastically rearrangements of orientation are needed for those entering water molecules. The growth processes of the water column lengths inside SWNTs with different charge distributions are also investigated, as shown in Figure 4. The simulations corresponding to the growth process were repeated 15 times for each system with different charge distributions, and the results were then

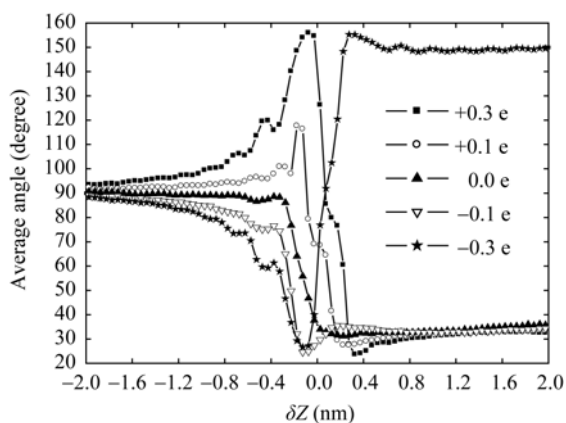


**Figure 3** Average dipole moment angular distributions for water molecules in the region near the lower end of SWNT with various charge distributions along the  $z$  direction. The orientation is detected by the angle between the SWNT axle and the water dipole moment, and the distance is measured from the lower end of the SWNT. The negative value stands for statistics in the water bath in front of the lower end of the SWNT, while the positive value stands for statistics within SWNT.

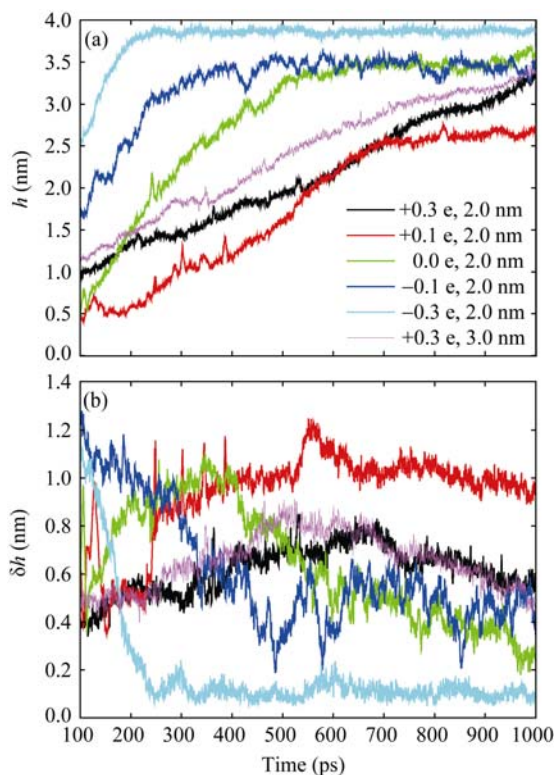


**Figure 4** The simulations corresponding to the growth process were repeated 15 times for each system with different charge distributions, and the results were then averaged. Water column lengths within SWNT (a) and the column length error distributions (b) for systems with various charge distributions and indenting depths evolve with time.

averaged. The error distributions for the growth column lengths inside SWNTs are shown in Figure 4(b). Gener-

ally, a positive charge modification to the SWNT's end would slow down the water column growth process, while the negative charge modification to the SWNT's end would, on the other hand, quicken the water column growth process. As shown in Figure 4(b), there exist regions showing relatively large water column length fluctuations for the case of positively charged and pristine SWNTs, these regions are corresponding to the time intervals in which the averaged water column height approximately reaches the outside surface water level, as shown in Figure 4(a), and these results are similar to our previous results<sup>[19]</sup>.

To further study these dynamic phenomena, the umbrella sampling technique and weighted histogram analysis method (WHAM) are used to obtain the free energy distributions in the process of water column growth for SWNTs with different charge distributions and indenting depths (Figure 5). These calculations show that to fill the water into the SWNTs until saturation is a thermodynamically spontaneous process. After prolonged simulation (generally around 2 ns), all water columns in various SWNTs finish their growth in our simulations, and the water column height approaches the saturation value and then fluctuates around it as shown in Table 1.

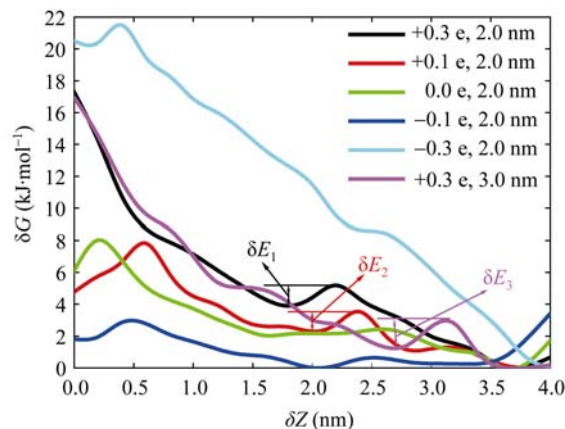


**Figure 5** The coarse free-energy curves as a function of the water column length inside SWNTs with different charge distributions and indenting depths. The energy barriers for cases with charges of +0.3 e and indenting depth of 2 nm, charges of +0.1 e and indenting depth of 2 nm, and charges of +0.3 e and indenting depth of 3 nm are  $\delta E_1$ ,  $\delta E_2$  and  $\delta E_3$  respectively.

From a dynamic view, it is obvious that the growth rate of water column inside the negatively charged SWNT is higher than that inside the uncharged SWNT. For example, in the case of  $-0.1$  e charge distribution,

the theoretical saturation height of water column inside SWNT corresponding to the minimal point in free energy curves is lower than the heights of SWNTs with the other charge distributions. At the same time, the free energy curve is relatively flat at the locations near the water column saturation height, thus providing relatively large freedom for the fluctuation of water column, as shown in Table 1. In the system with  $-0.1 e$  charge distribution, when the configuration effect of water molecules is included in the PMF calculation, the height of the free energy curve near the mouth range of the SWNT is the lowest, which corresponds to the most smooth variation of the dipole moment orientation for the entering water molecules, as shown in Figure 3. This is also the reason for relatively rapid filling rate of water molecules for SWNT decorated with  $-0.1 e$ . For the other cases, the increasing charge strength should normally increase the height of the free energy curve near the mouth range of the SWNT.

For the positively charged and pristine SWNTs, an energy barrier corresponding to the outside water surface level appears in the free energy curve, and this singularity of free energy variation tends to enhance the fluctuation of water column length in the growth process, as shown in Figure 4(b). The energy barriers for the case of the positively charged SWNTs (the value range of  $\delta E_i$  shown in Figure 5 is 1.2–1.3 kJ/mol) are apparently larger than those for the case of the pristine SWNT, as a result, the growth rate of water column inside the positively charged SWNT is slowed down. For the case of  $+0.1 e$  charge distribution, the average water column height maintains at around 2.5 nm after 700 ps, as shown in Figure 4(a), and the corresponding height fluctuation is also relatively large and at the same time shows little trend of decrease in height fluctuation before 1 ns, as shown in Figure 4(b). These convince us that there exists a local energy barrier near the location (around 2.5 nm), and some samples (actually 6 samples in our simulations) in the 15 independent simulations did not cross over this energy barrier ( $\delta E_2$  in Figure 5) until 1 ns.

To confirm the relationship between the location of the energy barrier and the outside water surface level, we have tried to change the indenting depth of SWNT

from 2.0 nm to 3.0 nm. When the maximal indenting depth is changed, the location of energy barrier varies with the outside surface water level, as shown in Figure 5. The results shown in Figures 4 and 5, indicate that the localized charge distribution (particularly on terminated carbon atoms) can clearly affect the overall dynamic properties of water transportation in the nanosized channels, unlike the size constraint imposing its effect mainly on the structural properties of water clusters confined<sup>[19]</sup>.

## 4 Conclusion

The charge modification to carbon nanotube would drastically affect the dynamical process of water transport within the CNT's channel. When positive charges are distributed over the lower end of SWNT, the water column growth inside the channel would be slowed down. On the other hand, negative charge modification to the SWNT would obviously increase the water column growth rate. The introduction of charge modification not only changes the interaction between the water cluster and the SWNT, but also leads to structural rearrangement of the water molecules. This is demonstrated in the calculation of the free energy, and these free energy curves clearly reflect the dynamical properties of water transport. The umbrella sampling and WHAM techniques are employed to obtain the free energy curves in the process of water column growth for SWNTs with different charge distributions and indenting depths. The obtained free energy curves support the conclusion that water column growth inside the negatively charged SWNT is faster than that in the pristine SWNT, and the fluctuation level of water column around saturation height inside SWNTs with different charge distributions can also be estimated. Results showed that the energy barrier located at the outside surface water level will be enhanced by the introduction of positive charges to the lower end of CWNT, and this increased energy barrier would slow down the water column growth. There also exists a correlation between the energy barrier location and the outside water surface level, that is, the energy barrier peak location is closely linked to indenting depth of SWNT.

1 Zhu F, Schulten K. Water and proton conduction through carbon nanotubes as models for biological channels. *Biophys J*, 2003, 85: 236–244

2 Kalra A, Garde S, Hummer G. Osmotic water transport through carbon nanotube membranes. *Proc Natl Acad Sci*, 2003, 100: 10175–10180

- 3 Corry B. Designing carbon nanotube membranes for efficient water desalination. *J Phys Chem B*, 2008, 112: 1427–1434
- 4 Preston GM, Carroll TP, Guggino WB, Agre P. Appearance of water channels in xenopus oocytes expressing red cell CHIP28 protein. *Science*, 1992, 256: 385–387
- 5 O'Connell M J, Bachilo S M, Huffman C B, Moore V C, Strano M S, Haroz E H, Rialon K L, Boul P J, Noon W H, Kittrell C, Ma J, Hauge R H, Weisman R B, Smalley R E. Band gap fluorescence from individual single-walled carbon nanotubes. *Science*, 2002, 297: 593–596
- 6 Miller S A, Young V Y, Martin C R. Electroosmotic flow in template-prepared carbon nanotube membranes. *J Am Chem Soc*, 2001, 123: 12335–12342
- 7 Huanga B, Xia Y, Zhao M, Li F, Liu X, Ji Y, Song C. Distribution patterns and controllable transport of water inside and outside charged single-walled carbon nanotubes. *J Chem Phys*, 2005, 122: 084708
- 8 Zimmerli U, Gonnet P G, Walther J H, Koumoutsakos P. Curvature induced L-defects in water conduction in carbon nanotubes. *Nano Lett*, 2005, 5: 1017–1022
- 9 Truskett T M, Debenedetti P G, Torquato S. Thermodynamic implications of confinement for a waterlike fluid. *J Chem Phys*, 2001, 114: 2401–2418
- 10 Brovchenko I, AlfonsGeiger, Oleinikova A. Water in nanopores: II. The liquid-vapour phase transition near hydrophobic surfaces. *J Phys: Condens Matter*, 2004, 16: S5345–S5370
- 11 Galloa P, Rovere M, Spohr E. Glass transition and layering effects in confined water: A computer simulation study. *J Chem Phys*, 2000, 113: 11324–11335
- 12 Gordillo M C, Marti J. High temperature behavior of water inside flat graphite nanochannels. *Phys Rev B*, 2007, 75: 085406
- 13 Hummer G, Rasaiah J C, Noworyta J P. Water conduction through the hydrophobic channel of a carbon nanotube. *Nature*, 2001, 414: 188–190
- 14 Koga K, Gao G T, Tanaka H, Zeng X C. Formation of ordered ice nanotubes inside carbon nanotubes. *Nature*, 2001, 412: 802–805
- 15 Takaiwa D, Hatano I, Koga K, Tanaka H. Phase diagram of water in carbon nanotubes. *Proc Natl Acad Sci*, 2008, 105: 39–43
- 16 Striolo A. The mechanism of water diffusion in narrow carbon nanotubes. *Nano Lett*, 2006, 6: 633–639
- 17 Gordillo M C, Marti J. Hydrogen bond structure of liquid water confined in nanotubes. *Chem Phys Lett*, 2000, 329: 341–345
- 18 Walther J H, Jaffè R, Halicioglu T, Koumoutsakos P. Carbon nanotubes in water: structural characteristics and energetics. *J Phys Chem B*, 2001, 105: 9980–9987
- 19 Meng L, Li Q, Shuai Z. Effects of size constraint on water filling process in nanotube. *J Chem Phys*, 2008, 128: 134703
- 20 Noon W H, Ausman K D, Smalley R E, Ma J. Helical ice-sheets inside carbon nanotubes in the physiological condition. *Chem Phys Lett*, 2002, 355: 445–448
- 21 Hanasakia I, Nakatanib A. Hydrogen bond dynamics and microscopic structure of confined water inside carbon nanotubes. *J Chem Phys*, 2006, 124: 174714
- 22 Werder T, Walther J H, Jaffè R L, Halicioglu T, Noca F, Koumoutsakos P. Molecular dynamics simulation of contact angles of water droplets in carbon nanotubes. *Nano Lett*, 2001, 1: 697–702
- 23 Vaitheeswaran S, Yin H, Rasaiah J C, Hummer G. Water clusters in nonpolar cavities. *Proc Natl Acad Sci*, 2004, 101: 17002–17005
- 24 Kutana A, Giapis K P. Atomistic simulations of electrowetting in carbon nanotubes. *Nano Lett*, 2006, 6: 656–661
- 25 Feng L, Zhang Z, Mai Z, Ma Y, Liu B, Jiang L, Zhu D. A Super-hydrophobic and super-oleophilic coating mesh film for the separation of oil and water. *Angew Chem Int Ed*, 2004, 43: 2012–2014
- 26 Feng X, Zhai J, Jiang L. The fabrication and switchable superhydrophobicity of TiO<sub>2</sub> nanorod films. *Angew Chem Int Ed*, 2005, 44: 5115–5118
- 27 Jiang L, Zhao Y, Zhai J. A lotus-leaf-like superhydrophobic surface: A porous microsphere/nanofiber composite film prepared by electrohydrodynamics. *Angew Chem Int Ed*, 2004, 43: 4338–4341
- 28 Wang S, Feng X, Yao J, Jiang L. Controlling wettability and photochromism in a dual-responsive tungsten oxide film. *Angew Chem Int Ed*, 2006, 45: 1264–1267
- 29 Leach A R. *Molecular Modelling: Principles and Applications*. 2nd ed. Upper Saddle River: Prentice-Hall, 2001
- 30 Kosztin I, Barz B, Janosi L. Calculating potentials of mean force and diffusion coefficients from nonequilibrium processes without Jarzynski's equality. *J Chem Phys*, 2006, 124: 064106
- 31 Torrie G M, Valleau J P. Nonphysical sampling distributions in Monte Carlo free-energy estimation: Umbrella sampling. *J Comp Phys*, 1977, 23: 187–199
- 32 Wan R, Li J, Lu H, Fang H. Controllable water channel gating of nanometer dimensions. *J Am Chem Soc*, 2005, 127: 7166–7170
- 33 Lindahl E, Hess B, van der Spoel D. GROMACS 3.0: a package for molecular simulation and trajectory analysis. *J Mol Mod*, 2001, 7: 306–317
- 34 van der Spoel D, Lindahl E, Hess B, van Buuren AR, Apol E, Meulenhoff PJ, Tieleman D P, Sijbers A, Feenstra K A, Drunen R V, Berendsen H. *Gromacs User Manual*. version 3.3 ed. 2005
- 35 Darden T, York D, Pedersen L. Particle mesh Ewald: An  $W \log(N)$  method for Ewald sums in large systems. *J Chem Phys*, 1993, 98: 10089–10092
- 36 Essmann U, Perera L, Berkowitz M L, Darden T, Lee H, Pedersen L G. A smooth particle mesh Ewald method. *J Chem Phys*, 1995, 103: 8577–8593
- 37 Frisch M J, Trucks G W, Schlegel H B, Scuseria GE, Robb MA, Cheeseman JR, Montgomery JA, Jr, Vreven T, Kudin KN, Burant JC, Millam JM, Iyengar SS, Tomasi J, Barone V, Mennucci B, Cossi M, Scalmani G, Rega N, Petersson GA, Nakatsuji H, Hada M, Ehara M, Toyota K, Fukuda R, Hasegawa J, Ishida M, Nakajima T, Honda Y, Kitao O, Nakai H, Klene M, Li X, Knox JE, Hratchian HP, Cross JB, Adamo C, Jaramillo J, Gomperts R, Stratmann RE, Yazyev O, Austin AJ, Cammi R, Pomelli C, Ochterski JW, Ayala PY, Morokuma K, Voth GA, Salvador P, Dannenberg JJ, Zakrzewski VG, Dapprich S, Daniels AD, Strain MC, Farkas O, Malick DK, Rabuck AD, Raghavachari K, Foresman JB, Ortiz JV, Cui Q, Baboul AG, Clifford S, Cioslowski J, Stefanov BB, Liu G, Liashenko A, Piskorz P, Komaromi I, Martin RL, Fox DJ, Keith T, Al-Laham MA, Peng CY, Nanayakkara A, Challacombe M, Gill PMW, Johnson B, Chen W, Wong MW, Gonzalez C, Pople J A. *Gaussian 03*. Revision E.01 ed. Pittsburgh PA: Gaussian, Inc. 2007
- 38 Won C Y, Joseph S, Alurua N R. Effect of quantum partial charges on the structure and dynamics of water in single-walled carbon nanotubes. *J Chem Phys*, 2006, 125: 114701